The role of estrogen in the regulation of neutrophil granulocyte szuperoxide production and the proliferation of MCF7 breast cancer cells

Theses

István Marczell MD

Semmelweis University
Doctoral School of Clinical Medicine

Supervisor: Gábor Békési MD PhD

Opponents: Nóra Hosszúfalusi MD PhD
Erika Hubina MD PhD

President of PhD Theoretical Exam Committee:
Anna Blázovics MD DSc

Members of Phd Theoretical Exam Committee:
Péter Vajdovich MD PhD
Zoltán Kukor MD PhD

Budapest
2019

Table of contents

Introduction

The current understanding of steroid actions is the result of several decades of scientific work. In 1960 Clever and Karlson published their results about the steroid molecule ekdizon that induced the „swelling" of the DNA in insect larvae. Decades later the modern era of steroid hormones began with the recognition that intracellular steroid hormones act as ligand activated transcription factors, thereby responsible for a wide range of genetic effects. As early as 1942 János Selye described however, that intraperitoneal administration of progesterone has an immediate anaesthetic effect on rats that cannot be explained with transcriptional effects. Today we see steroid signaling as the cooperation of different receptor systems, including membrane bound and intracellular steroid receptors that orchestrate the cells response to various steroids.

Regarding membrane bound estrogen receptors, there are at least two structurally different receptor groups. The membrane bound form of the classical nuclear estrogen receptor – called mER – is the same gene product as ERα. As a post-translational modification the protein is palmitoylated by the DHHC7 and DHHC21 palmitoyl-acil-transferase enzymes. This modification allows the receptor to be anchored to the cell membrane, where it resides in membrane invaginations called caveolae. Here the receptor – with other proteins - form a signaling complex, called signalosome. This complex regulates different physiological processes, amongst which endothelial NO synthesis is probably the most important. The other structurally different estrogen membrane receptor is called GPER and it is a G-protein coupled membrane receptor.

In the thesis I discuss estrogen signaling in two different models focusing in both on the role of non-classical estrogen signaling. In the first introduced model we aimed to quantify the contribution of membrane estrogen signaling to the overall proliferative effect of estrogen on breast cancer cells. Estrogen dependency of ductal carcinoma cells render estrogen signaling a particularly important field of research in this setting. In the second model we investigated the pathway that mediates the antioxidant effect of estrogen in fMLP stimulated neutrophil granulocytes. The immediate non-genomic anti-inflammatory effect of estrogen on neutrophil granulocytes is described by several groups, and it is recognized as an important factor in the vasculoprotective effect of estrogen.

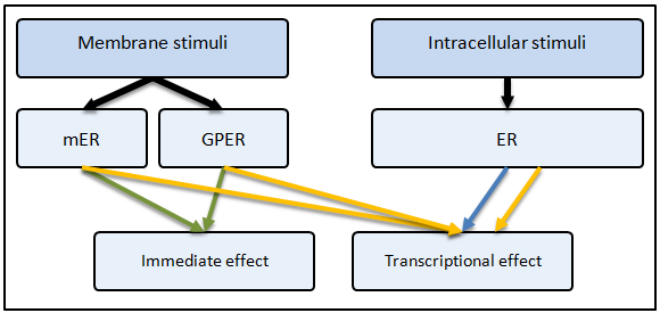

Figure 1.
Classification of estrogen effects
Green arrow indicates the short term effects of estrogen treatment, while yellow and blue arrows represent intermediate and long term effects accordingly. (mER –membrane associated classical estrogen receptor, GPER - G-protein coupled estrogen receptor, ER estrogen receptor (nuclear))

Aims

In my thesis I was searching answer to the following questions:

1. What genes would be suitable for monitoring the proliferative effects of estrogen in MCF7 breast cancer cells?
2. How the expression of these genes is altered by 17β-estradiol, the membrane impermeable estrogen-BSA and the GPER selective G1?
3. Can the phenomenon of ligand mediated receptor internlaization be observed in case of membrane associated estrogen receptors?
4. If it does, how the inhibition of the internalization process alters the proliferative effects of estrogen in breast cancer cells?
5. What pathway mediates the antioxidant effect of estrogen in fMLP stimulated neutrophil granulocytes?

Methods

Methods used during the experiments with the MCF7 cells

Cell culturing

Human breast carcinoma MCF-7 cell line was obtained from the cell bank of the 2nd Department of Pathology, Semmelweis University. Cells were grown in RPMI-1640 medium (Sigma-Aldrich, Cat. No.:R8758-500ML) supplemented with 10% fetal bovine serum, 100 U/mL penicillin and 100 μg/mL streptomycin in a humidified incubator at

37 °C with 5% CO_2. Prior to treatments, cells were cultured in serum and antibiotic free medium for 24 hours.

Treatments

E2-BSA (Sigma-Aldrich, V St. Louis, MO, USA) was dissolved in phosphate-buffered saline (PBS), and free estradiol was removed by filtration using the technique described by Stevis et al. The filtered solution was added to serum and antibiotic free medium. Treatments were carried out in 3 different concentrations (10^{-10}M, 10^{-9}M, 10^{-8}M), and each group consisted of three samples. Estrogen concentrations were calculated with 30 mol steroid per mol bovine serum albumin (BSA) according to manufacturer's specifications.

17β-estradiol (Sigma-Aldrich, St. Louis, MO, USA) was dissolved in ethanol then added to serum and antibiotic free medium in the same three concentrations (10^{-10}M, 10^{-9}M, 10^{-8}M). G1 (Tocris Bioscience, Bristol, UK) was dissolved in dimethyl sulfoxide (DMSO) in the final concentration of 10^{-8} M. Dynasore (Sigma-Aldrich,**)** was dissolved in DMSO and used in 80 μmol treatment concentration, and was applied 30 minutes prior to subsequent 17β-estradiol treatment (in 10^{-10}M concentration). All treatments were performed in triplicate. The reagents were added to the cell media for 3 hours with the same dissolvent, and then cells were collected and kept at -80 ˚C in Trizol® Reagent (Applied Biosystems, Life Technologies, Carlsbad, California, US) until further processing.

Gene Expression Studies

Re-analysis of gene expression studies available in microarray data repositories

Microarray data were downloaded from Gene Expression Omnibus (GEO; http://www.ncbi.nlm.nih.gov/geo/). Four time-course studies with a total of 18 arrays were selected for further analysis (see Supplementary Table Sheet 1). The treatment period was 3 or 4 hours for all samples. Two common gene chip families (Affymetrix U133 and U133 Plus 2.0) were used in these experiments. There are 22,277 common probe sets between the two array types that map 13,186 genes. For the meta-analysis, the common probe sets across the platforms were used. All data were normalized with the Guanine Cytosine Robust Multi-Array Analysis (GCRMA) method.

The statistical significance of the results was evaluated by the non-parametric algorithm 'Rank products', available as the 'RankProd' package at Bioconductor (http://www.bioconductor.org). This statistically robust method has been demonstrated as a reliable one for microarray data analysis. It detects genes that are consistently highly ranked in several replicated experiments, independently of their numerical intensities. The method ranks each feature within an experiment based on that features' score (in our case Log expression values), and then combines these ranks, instead of combining the data or p-values. The results are provided in the form of P values defined as the probability that a given gene is ranked in the observed position by chance. Differentially regulated probe sets were selected based on the estimated percentage of false positive predictions (pfp), which is equivalent to a false discovery rate. The pfp is calculated

using a permutation based procedure (50,000 permutations were conducted). Genes with a pfp of less than 0.05 were selected for further investigation (Supplementary Table Sheet 2.).
On GEO and ArrayExpress we found one microarray experiment consisting of 4 arrays carried out with estrogen-BSA treated MCF7 cells. Measurements were conducted with Affymetrix U133 Plus2 platform, and normalized with GCRMA. Statistical analysis was carried out using Student's t-test, and $p < 0.05$ was considered significant (Results can be found in Supplementary Table Sheet 3.).

Gene expression changes upon E2, E2-BSA, G1 and dynasore treatments
Total RNA was isolated from an average of $2x10^6$ MCF7 cells cultured in T-25 flasks. RNA purification was carried out using Trizol® Plus RNA Purification Kit (Life Technologies, Carlsbad, California, USA) according to the manufacturer's instructions. RNA content was determined using NanoDrop 2000 spectrophotometer. For each sample ~1000 ng RNA was transcribed to cDNA using High Capacity RNA-to-cDNA Kit Pre-designed TaqMan® Gene Expression Assays were used for real-time PCR (CCND1, ERBB2, GAPDH, CKNK5, KDM4B, MYC, RPL13A). We used GAPDH and RPL13A as housekeeping genes. Measurements were performed using TaqMan® Fast Advanced Master Mix with no UNG. The 7500 Fast Real-Time PCR System was used with the following parameters: 95°C for 20 seconds followed by 60 two-step cycles at 95°C for 3 seconds and at 60°C for 30 seconds. All RT-PCRs were performed in triplicate. SDS 1.3.1 software was used for calculation of the threshold cycle (Ct) values in each sample. For interpretation of the results, we applied the ddCT method. The results were adjusted to RPL13A as a selected housekeeping gene. Statistical analysis for single dose treatments (in our study treatments with G1 and co-treatment using dynasore with 17β-estradiol) were carried out using Student's t-test. Samples showed equal variance, and significance was considered at $p<0,05$.

Imaging studies
Preparation of semithin and ultrathin cryosections
For morphological examination control and treated MCF7 cells were fixed in freshly prepared 4% paraformaldehyde (PFA) in 0.1 M PB for 1 h at room temperature. The PFA fixed samples were placed and stored in 1 % paraformaldehyde (in 0.1 M PB) at 4 °C until further processing. For cryosectioning and immunolabeling, the fixed cells were subsequently detached with a scraper, washed twice in PBS and once in 0.02 M glycine/PBS by centrifugations at 1000 rpm for 10 min each at room temperature. The pellets were then infiltrated with 12% gelatine in PB at 37 °C for 10 min and then centrifuged with 1000 rpm at room temperature for 5 min. The samples were placed on ice for 30 min and afterwards cut into small blocks. For cryoprotection, the blocks were infiltrated with 2.3 M sucrose at 4 °C overnight and afterwards mounted on metal pins, frozen and stored in liquid nitrogen. For preparing semithin and ultrathin cryosections we used Leica Ultracut S ultramicrotome equipped with cryo-attachment (Vienna,

Austria). The pickup solution was a 1:1 mixture of 2.3 M sucrose and 1.8 % methylcellulose.

Immunolabeling for light and electron microscopy

The 0.7 μm semithin cryosections mounted on microscopic slides were incubated with 0.02 M glycine in PBS for 15 min and were blocked in PBS containing 1% BSA. Primary antibodies rabbit polyclonal anti-caveolin-1 antibody (1:200; BD, Transduction Laboratories, Lexington, KY) and rabbit polyclonal anti-ERα (H-184): sc-7207) antibody (1:200, Santa Cruz Biotechnology, Inc) were applied in 1% BSA containing buffer in a humidified chamber at 4 °C (overnight). Biotinylated anti-rabbit IgG (1:200; Vector Laboratories Inc, Burlington, CA) was applied as a secondary antibody for indirect immunolabeling when two polyclonal primary antibodies were used. For immunofluorescence visualization, Streptavidin Alexa Fluor conjugated to 488 (1:200) was used and for double immunolabeling the second primary antibody was visualized with goat anti-rabbit IgG Alexa Fluor 555 (1:200, MolecularProbes, Leiden, the Netherlands). The nuclei were stained with DAPI (Vector Laboratories Inc, Burlington, CA). The visualization was performed in a Bio-Rad (Zeiss, Budaörs, Hungary) Radiance 2100 Rainbow Confocal Scanning system coupled to a Nikon Eclipse E800 microscope (Nikon, Tokyo, Japan). Lasersharp 2000 6.0 software (Zeiss, Oberkochen, Germany) was used for image acquisition and final images were assessed using Adobe Photoshop 7.0. program (San Diego, CA, USA). (Only linear adjustments with respect to brightness and contrast were applied to the entire image that did not alter the interpretation of the original material.) Before double-immunolabeling all antibodies were rigorously tested for single labeling at different dilution. Negative controls were applied in each experiment to avoid false positive results. For cryosectioning and immuno-EM, the fixed tissues were further processed as described by Slot and Geuze.

Methods used during the experiments with neutrophil granulocytes

Cell separation:

Whole peripheral blood samples were obtained into EDTA-tubes, drawn from 4 female and 6 male donors, aged between 25 and 61. The blood was layered onto Ficoll for the sedimentation of red blood cells. It then was transferred to 63 and 72% Percoll and centrifuged for 25 min at a rate of 300g, on 20 °C. Granulocytes were separated as follows; they were washed twice with buffer and centrifuged at 220x g. Cells aggregated at the bottom of the tube were re-suspended in a few millilitres of Hank's salt solution (Life Technologies, Catalogue Number: 14025-050), and counted using Turk's solution. The cell concentration of the suspension was adjusted to 10^7/ml for the protein phosphorylation experiment and 5 x10^6/ml for every other measurement.

Protein phosphorylation and pathway identification:

Neutrophil granulocytes - separated as described above - were treated for 10 minutes with three different concentrations of 17-β-estradiol (10^{-10}, 10^{-9}, 10^{-7}M) (Sigma-Aldrich, Cat. No E8875), with and without a subsequent fMLP treatment (10^{-}

^{6}M) (Sigma-Aldrich, Cat. No.: F3506). The cell lysates were used for the kinase phosphorylation measurements.

Phosphorylations were measured using the Human Phospho-Kinase Antibody Array (from R&D Systems, Cat. No.:ARY003B) according to the manufacturer's instructions in order to quantify the neutrophil granulocyte response to estrogen and fMLP treatments. Briefly, the array contains nitrocellulose membrane bound capture antibodies against 43 different signaling molecules. Cell lysates are applied to the membrane, then the array is washed to remove unbound proteins, followed by incubation with a mixture of biotinylated detection antibodies. Streptavidin-HRP and chemiluminescent detection reagents are applied and a light signal is produced at each capture spot corresponding proportionally to the amount of phosphorylated protein bound. Each membrane set contained one untreated control and three treated samples. Every measurement was carried out in duplicate. For the evaluation of the capture spot intensities we used the ICY Bioimage Analyzer software and the background noise reduction protocol suggested by the manufacturer of the array. For statistical evaluation we used the two-sample t-test, a change was considered significant $p<0.05$

During the pathway analysis we selected the phosphorylation changes that were significantly altered in the same direction in at least two of all three concentrations compared to the control. The list of these proteins is shown on Figure 5. The protein lists were loaded into the Ingenuity Pathway Analyser (IPA, Ingenuity Systems, www.ingenuity.com; Redwood City, CA, USA) for the identification of the affected pathways using core analysis function and the pathway library. Amongst the top search results the fMLP and estrogen pathways were selected arbitrarily and amended manually using data derived from STRING (Search Tool for the Retrieval of Interacting Genes/Proteins; http://string-db.org/) and literature research. The proposed connection between estrogen and fMLP induced pathways are shown in Figure 6. Protein interactions shown have been exported from Ingenuity Pathway Analyser.

fMLP stimulation and superoxide production:

The chemotactic bacterial peptide fMLP (N- Formylmethionine-leucyl-phenylalanine) stimulated superoxide production was measured by photometry using Quarnieri's method as modified by Jansson (Guarnieri, Melandri et al. 1990; Jansson 1991). The reduction of ferricytochrome-C (Sigma-Aldrich, Cat. No.: C-7752) by superoxide was measured as optical density (OD). Superoxide anion production was assessed as change of optical density (Δ OD) 5 minutes after stimulation.

In the first part of this experiment isolated neutrophils were treated with 17-β-estradiol (10^{-9}M) for ten minutes then stimulated with fMLP (10^{-6}M). In the second part, kinase inhibitors (Akt inhibitor, Src inhibitor, Vichem Ltd. Cat. No.: VCC374536:01, VCC291860:24; Rac1 inhibitor – Gentaur Ltd., Cat. No.: NSC 23766.) were used in the recommended concentrations, dissolved in DMSO and applied for 20 minutes prior to estradiol treatment. In order to rule out any potential interference with the results we added DMSO in the same concentration to all samples.

For each study group 5-8 measurements were carried out, the results were interpreted as percentages of the control which was considered 100%. Each statistical analyses were done using Statistica 7.0 (StatSoft Inc. Tulsa, USA) For statistical evaluation we used Student's test, a change was considered significant $p<0.05$ (Figure 7.)

Results

Experiments with MCF7 cells

Re-analysis of gene expression studies available at microarray data repositories

Out of the 22,277 probe sets, we identified 378 at 3 or 4 h time point, with a very strict false discovery rate of $pfp \leq 0.05$ (see methods). By mapping the probe sets to genes, we have identified 285 unique upregulated and 49 downregulated genes that were differentially expressed (All results obtained from microarray meta-analysis are available in Supplementary Table Sheet 1.) The selected key genes (KCNK5, KDM4B, MYC and CCND1) were all significantly upregulated while ERBB2 (HER2) was downregulated, although its expression change was not significant compared to untreated cells. We further focused on the expression of the above mentioned five genes as their expression has already been extensively studied and all have been confirmed as a target of E2.

Statistical analysis of the microarray data of estrogen-BSA treatment identified 586 genes with significantly altered expression. MYC, KDM4B, and KCNK5 were significantly upregulated after 3 hours of estrogen-BSA treatment. The expression change of CCND1 did not reach statistical significance similarly to the downregulated ERBB2.

Validation of gene expression changes upon E2, E2-BSA, G1 and dynasore treatments by qRT-PCR

Upon 17β-estradiol treatment, the expression of all genes selected from microarray studies was significantly upregulated (Fig. 1A). Membrane receptor selective estrogen-BSA (mER) treatment also upregulated remarkably the expression level of all these genes and this change was similar or even stronger for KCNK5 and KDM4B compared to those observed with 17β-estradiol treatment. (Fig. 1B). Dynamin inhibitor, dynasore pretreatment abolished the effect of 17β-estradiol on all genes except of KCNK5 but its expression was also significantly lower than measured after 17β-estradiol treatment (Fig 1A).

In order to dissect the mERα signaling from GPER signaling, we treated MCF-7 cells with G1, a selective GPER agonist. G1 treatment of MCF7 cells resulted only moderate effect on expression of the studied genes. Significant effect was observed for KCNK5 only (Fig. 2.). Numerical ddCT values are shown in Supplementary Table Sheet 5.

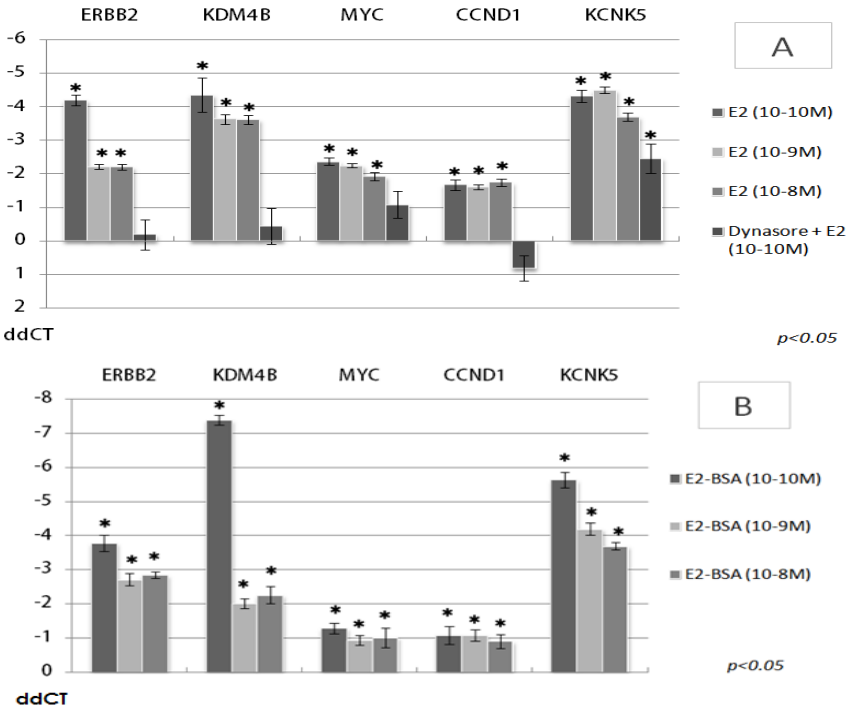

Figure 2.

Gene expression changes after treatment of MCF7 cells with 17β-estradiol and estrogen-BSA.

Expression changes of CCND1, ERBB2, KCNK5, KDM4B and MYC after 17-β-estradiol (E2) (A) and estrogen-BSA treatment (B). Treatments were performed in three different concentrations (10^{-10}M, 10^{-9}M, 10^{-8}M) and a similar E2 treatment (10^{-10}M) on dynamin inhibitor (dynasore, 30 min) pretreated cells. Y-axis represents ddCT values, 0 line indicates control level. (Error bars represent standard deviation, asterisks indicate significant changes compared to control with p value <0,05). Numerical ddCT values are shown in Supplementary Table Sheet 5.

Imaging studies

We examined ERα distribution in control and treated MCF7 cells using fluorescence immunolabeling. We detected ERα signals both inside the nucleus as well as in the cytoplasm of MCF7 cells under control conditions (Fig 3A). Upon E2 treatment the majority of receptor labeling accumulated inside the nucleus, while after estrogen-BSA stimulation ERα could be observed predominantly in the cytoplasm and to a lesser extent in the plasma membrane (Fig. 3B-C.)

In order to prove that plasma membrane ERα pool resides in caveolin-1 positive lipid rafts, we carried out double immunolabeling. Our result showed several orange puncta indicating co-labeling of caveolin-1 and ERα. This could be observed both along the plasma membrane as well as in the cytoplasm. Fig. 4A-C).

Further, we examined the morphological effect of combined dynasore and estrogen treatment of MCF7 cells with immunoelectron microscopy. After dynasore treatment, ERα labeling occurred in distorted, elongated caveolin-1 positive structures right beneath the cytoplasm. The deeper cytoplasmic areas lacked caveolin-1 positive vesicular structures suggesting that endocytosis via this route was disturbed (Figure 4D).

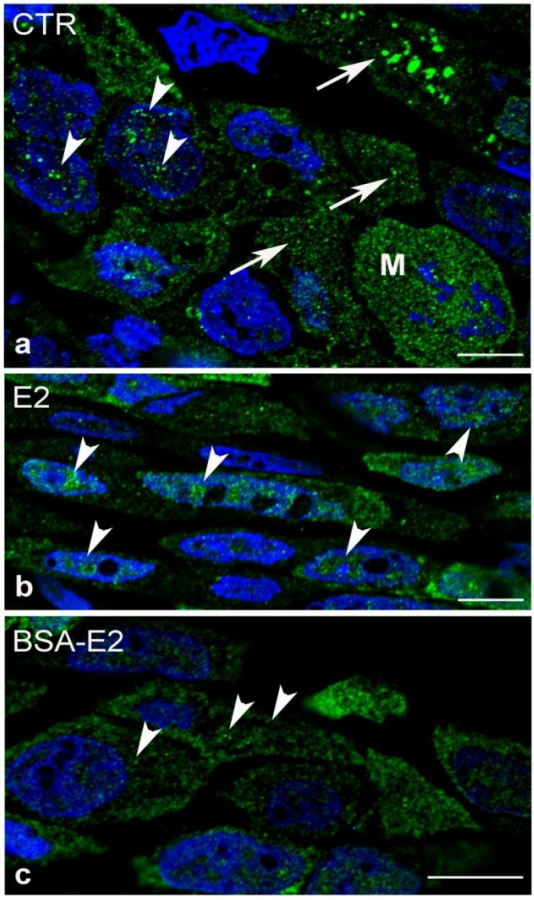

Figure 3.
ER-α labeling of control and treated MCF7 cells on semithin frozen sections.
*A**.)** ER-α receptor labeling occurred in aggregates or as punctate structures both inside the nucleus (arrowheads) as well as in the cytoplasm of untreated MCF7 cells. Observe a mitotic form (M) where intensive ERα expression could be detected. B**.)** Upon E2 treatment (2 min, 10^{-8} M/l), the majority of receptor labeling accumulated inside the nucleus (arrowheads). **C.)** Immunofluorescence labeling of ER-α could predominantly be observed in the cytoplasm and submembranous localization of MCF7 cells upon BSA-E2 treatment (arrowheads). Nuclei were stained with DAPI, bars indicate 10μm.*

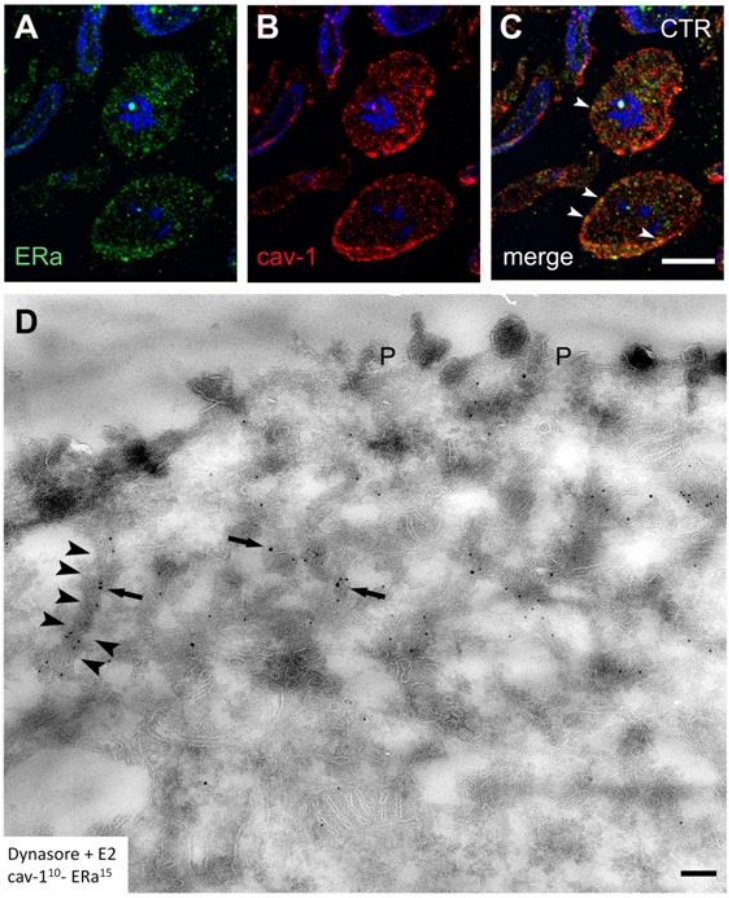

Figure 4.
Morphological changes upon combined Dynasore- E2 treatment of MCF7 cells.
Semithin frozen sections of control MCF7 cells labeled with antibodies directed against ER-α (green) and caveolin-1 (red). ***A-C:*** *ER-α receptor labeling occurred inside the cytoplasm and the plasma membrane in MCF7 cells. Nuclear occurrence of the receptor could also be observed, however, to a lesser extent. The merged image of ER-α and caveolin-1 double labeling shows overlapping areas at the plasma membrane (arrowheads), while intracytoplasmic co-labeling could also be detected. Bars indicate 10 μm, nuclei were stained with DAPI.* ***D:*** *Ultrathin cryosection shows morphologically distorted, elongated caveolae (arrowheads) indicating the effect of Dynasore treatment. Larger gold particles labeling ER-α could be observed in the close vicinity of caveolin-1 positive structures right beneath the plasma membrane (P). Note that the deeper cytoplasmic areas lack both small (ERα) and larger (caveolin-1) gold particles indicating the disturbed internalization of caveolin-1 positive vesicles. Bar indicates 200nm.*

Experiments regarding neutrophil granulocyte function

Proteome Profiler Phosphorylation Array

In the protein phosphorylation experiment we measured the phosphorylation state of 43 different second messengers after estrogen and/or fMLP treatment.

The estrogen (E2) treatments were carried out in three different concentrations (10^{-10}, 10^{-9}, 10^{-7}M). According to the pathway identification the detected phosphorylation changes affected mostly known estrogen pathways (Figure 6.). In other words most messengers that showed significant change were involved in routes that are related to non-genomic estrogen action - according to the used pathway libraries. Other significant changes could also be related to more remote estrogen effects. Most other significant changes are also related to estrogen action. AMPKα1 activation by estrogen is takes place via the Ca^{2+}/calmodulin-dependent protein kinase kinase β (Gayard, Guilluy et al. 2011; Yang and Wang 2015), Pyk2 (Moro, Reineri et al. 2005), Plc-γ1(Qiu, Ronnekleiv et al. 2008), STAT3(Guo, Zhang et al. 2011), Erk1/2 and JNKs (Lorenzo 2003), p38 (Lee and Bai 2002), MSK1/2 (Roux and Blenis 2004))

(Lee and Bai 2002; Lorenzo 2003; Roux and Blenis 2004; Moro, Reineri et al. 2005; Qiu, Ronnekleiv et al. 2008; Gayard, Guilluy et al. 2011; Guo, Zhang et al. 2011)

We performed a measurement with fMLP treatment only, in order to identify the significant phosphorylation changes. Almost every change was involved in the fMLP induced inflammatory pathway however the kit measures only relatively small portion of these messengers (Fumagalli, Zhang et al. 2007; Osterloh, Geisinger et al. 2009; Tang, Zhang et al. 2011). (Results are not shown)

Combined estradiol and fMLP treatments were carried out in the known three 17-β-estradiol concentrations. The induced phosphorylation changes corresponded to the summation of the two previous measurements, although some estrogen induced changes did not reach the level of significance in the combined treatment. On the other hand, compared to estrogen treatment five new messenger proteins showed significant phosphorylation change (GSK3, HSP60, PDGFRβ, mTOR). GSK3, HSP60, mTOR are all involved in the fMLP induced activation of neutrophil cells, while platelet derived growth factor receptor (PDGFRβ) may function as a chemoattractant receptor (Shure, Senior et al. 1992) but its role is unknown regarding fMLP. Results are shown in Figure 5. (Kwon, Kwon et al. 2000; Taylor, Richter et al. 2012)

Second messenger	Control	E2(10^{-10}M)	E2(10^{-9}M)	E2(10^{-7}M)
Akt (at S473)	1751.0	2858.00	5275.00	2828.00
Akt (at T308)	3729.00	4569.00	7585.00	6290.00
AMPKα1	1269.50	3771.50	2686.00	4040.50
c-JUN	1297.80	4124.00	2331.00	2404.80
ERk1/2	0.00	94.00	2173.00	1362.00
Hck	0.00	343.50	2980.00	2503.00
JNK pan	925.50	4708.00	4323.00	3553.00
MSK1/2	667.50	1432.50	2768.00	4111.50
p38a	0.00	164.00	4306.50	2711.00
p53	2389.00	4197.00	5595.00	3345.00
PLC-γ 1	617.80	4109.00	2714.80	2807.80
PYK2	1159.80	6019.00	3183.00	3211.80
Src	1427.00	1951.00	2913.00	3215.00
STAT3	2940.00	133.25	35.65	117.15
STAT6	2750.50	3148.50	5475.50	3643.50

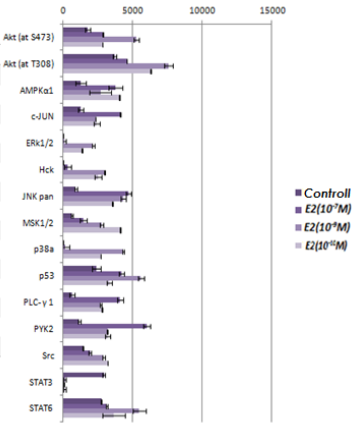

Second messenger	Control	E2+fmlp(10^{-10}M)	E2+fmlp(10^{-9}M)	E2+fmlp(10^{-7}M)
Akt (S473)	65.5	218.5	1305.3	909.3
Akt (T308)	3712.8	5302	4639.5	10491.25
AMPKα1	1384.5	4019	6694.8	4147.3
ERk1/2	0	1139	2253.3	538.3
GSK-3a/b	6275.5	9446	10553.8	8411.3
HSP60	1300.3	3495	3095.5	6852.25
JNK pan	2460.5	6631	9875.8	6837.8
MSK1/2	10443.5	13723	14841.8	10582.8
p38a	357	1054	1221.8	363.8
PDGFR beta	3408.5	4139	6826.3	3667.80
Src	4413	5076	7055.8	4581.8
STAT3	1585.3	2727	2367.5	6645.75
TOR	7652.5	10579.5	10497.3	7956.3

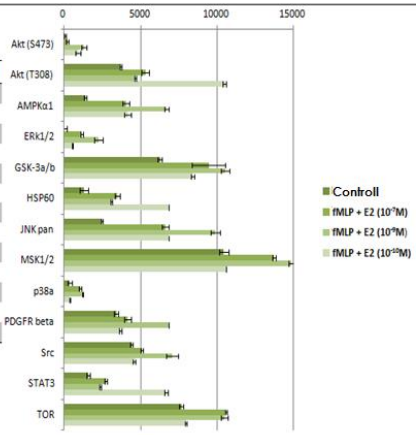

Figure 5.

Selected significant phosphorylation changes

Different marks represent the signal intensity values of selected, significant (*) phosphorylation changes after (a) 17-β-estradiol treatments, (b) fMLP with 17-β-estradiol treatments. Using this phosphorylation data we managed to identify certain estrogen induced signaling pathways.

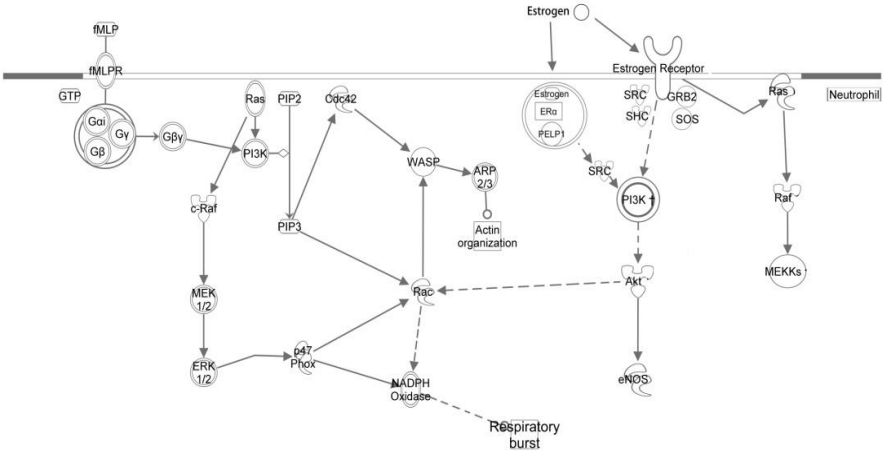

Figure 6.

Schematic diagram of the identified pathway

The diagram shows fMLP and estrogen initiated pathways and their connection. The identified functional pathway is indicated with dashed arrows. Estrogen induces diverse phosphorylation changes, the proposed PI3K mediated activation takes place mostly via estrogen membrane receptors however there are data about nuclear receptor initiated activation as well.

Superoxide production and kinase inhibitors

As it has been shown before by others (Abrahams, Collins et al. 2003) and our study group as well (Bekesi, Tulassay et al. 2007) 17-β-estradiol decreases the bacterial peptide fMLP induced superoxide production of human neutrophil granulocytes. In our experiment we use superoxide production as an indicator of estrogen effect on chemoattractant induced free radical production. Using specific inhibitors of the second messengers in the identified pathway we measured the fMLP stimulated superoxide production (Figure 7.).

Akt and Src inhibitors significantly increased the superoxide production antagonising the decreasing effect of estrogen. This result therefore suggests that the proposed pathway is involved in the mediation of estrogen effect. Rac1 participates in the assembly and activation of the NADPH oxidase (NOX) complex, the enzyme mainly responsible for phagocyte superoxide production. As expected then the inhibition of Rac1 led to a significant decrease in superoxide production compared to the estrogen treated samples. This indicates that Rac1 is an important regulatory point in the process of the oxidative burst and superoxide production.

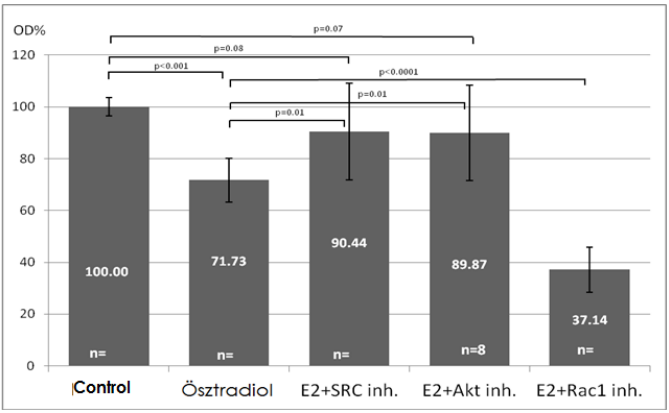

Figure 7.

Effects of messenger inhibitors on superoxide production with optical densitometry

Inhibitors of the estrogen initiated pathways abolish the superoxide reducing effect of estradiol. Only Rac1 inhibition increases it – which is in line with our prior expectations. Y-axis shows the mean optical density (OD) values that are shown as percentage of control.

Conclusions

Summarizing our data we concluded:

1. Meta-analysis of all available microarray data CCND1, ERBB2, KCNK5, KDM4B and MYC are available to monitor the proliferative effect of estrogen..

2. 17β-estradiol and E2-BSA significantly increase the expression of all the monitored genes. The GPER specific agonist G1 on the other hand had significant effect only in the case of KCNK5

3. Our imaging studies revelaed that mER shows ligand mediated internalization in MCF7 cells.

4. Inhibition of the internalization via dynamin abolishes the proliferative effect of estrogen.

5. The antioxidant effect of estrogen on fMLP stimulated neutrophil granulocytes is – at least partly – mediated via Rac1 inhibition.

Publications:

Publications in the topic of this thesis

I. Marczell I, Hrabak A, Nyiro G, Patocs A, Stark J, Dinya E, Kukor Z, Toth S, Tulassay Zs, Racz K, Bekesi G: 17-beta-estradiol Decreases Neutrophil Superoxide Production through Rac1. *Exp Clin Endocrinol Diabetes* 2016, 20:20.; PMID:27437916; DOI: 10.1055/s-0042-105556; IF:1,6

II. Marczell I, Balogh P, Nyiro G, L Kiss A, Kovacs B, Bekesi G, Racz K, Attila Patocs: Membrane-bound estrogen receptor alpha initiated signaling is dynamin dependent in breast cancer cells. *Eur J Med Res* 2018 Jun 7;23(1):31. doi: 10.1186/s40001-018-0328-7; IF:1,4

Other publications:

Módos Dezső, Bulusu Krishna C, Fazekas Dávid, Kubisch János, Brooks Johanne, Marczell István, Szabó Péter M, Vellai Tibor, Csermely Péter, Lenti Katalin, Bender Andreas, Korcsmáros Tamás: Neighbours of cancer-related proteins have key influence on pathogenesis and could increase the drug target space for anticancer therapies
NPJ SYSTEMS BIOLOGY AND APPLICATIONS 3:(1) Paper 2. (2017)

Stark J, Varbiro S, Sipos M, Tulassay Z, Sara L, Adler I, Dinya E, Magyar Z, Szekacs B, Marczell I, Kloosterboer HJ, Racz K, Bekesi G: Antioxidant effect of the active metabolites of tibolone GYNECOLOGICAL ENDOCRINOLOGY 31:(1) pp. 31-35. (2015)

Stark J, Varga Z, Ghidan A, Vajdovich P, Szombath D, Marczell I, Varbiro S, Dinya E, Magyar T, Tulassay Z, Szekacs B, Nagy K, Racz K, Bekesi G: The effect of indomethacin, myeloperoxidase, and certain steroid hormones on bactericidal activity: an ex vivo and in vivo experimental study. ANNALS OF CLINICAL MICROBIOLOGY AND ANTIMICROBIALS 13:(1) Paper 27. 9 p. (2014)

Szabo DR, Baghy K, Szabo PM, Zsippai A, Marczell I, Nagy Z, Varga V, Eder K, Toth S, Buzas EI, Falus A, Kovalszky I, Patocs A, Racz K, Igaz P: Antitumoral effects of 9-cis retinoic acid in adrenocortical cancer. CELLULAR AND MOLECULAR LIFE SCIENCES 71:(5) pp. 917-932. (2014)

Stark J, Tulassay Z, Lengyel G, Szombath D, Szekacs B, Adler I, Marczell I, Nagy-Repas P, Dinya E, Racz K, Bekesi G: Increased total scavenger capacity in

rats fed corticosterone and cortisol on lipid-rich diet. ACTA PHYSIOLOGICA HUNGARICA 100:(1) pp. 84-88. (2013)

Adler I, Tulassay Z, Stark J, Marczell I, Nagy-Repas P, Varbiro S, Magyar Z, Szekacs B, Racz K, Bekesi G: The effect of certain steroid hormones on the expression of genes involved in the metabolism of free radicals. GYNECOLOGICAL ENDOCRINOLOGY 28:(11) pp. 912-916. (2012)

Békési G, Tulassay Z, Lengyel G, Schaff Z, Szombath D, Stark J, Marczell I, Nagy-Repas P, Adler I, Dinya E, Racz K, Magyar K: The effect of selegiline on total scavenger capacity and liver fat content: a preliminary study in an animal model
JOURNAL OF NEURAL TRANSMISSION 119:(1) pp. 25-30. (2012)

Marczell I, Tulassay Zs, Békési G, Tóth M, Patócs A, Stark J, Rácz K: A sejtfelszíni szteroidreceptorok szerepe és azok klinikai vonatkozásai. MAGYAR BELORVOSI ARCHIVUM 65:(5) pp. 289-297. (2012)

Magyar Z, Békési G, Rácz K, Fehér J, Schaff Zs, Lengyel G, Blázovics A, Illyés Gy, Szombath D, Hrabák A, Szekács B, Gergics P, Marczell I, Dinya E, Rigo J Jr., Tulassay Zs: Increased Total Scavenger Capacity and Decreased Liver Fat Content in Rats Fed Dehydroepiandrosterone and Its Sulphate on a High-Fat Diet GERONTOLOGY 57:(4) pp. 343-349. (2011)